Available online at www.sciencedirect.com
ScienceDirect
Trans. Nonferrous Met. Soc. China 25(2015) 46−53
Transactions of Nonferrous Metals Society of China
www.tnmsc.cn

Effect of iron addition on microstructure, mechanical and magnetic properties of Al-matrix composite produced by powder metallurgy route

A. FATHY[1], Omyma EL-KADY[2], Moustafa M. M. MOHAMMED[3]

1. Department of Mechanical Design and Production Engineering, Faculty of Engineering, Zagazig University, Zagazig 44519, Egypt;
2. Powder Metallurgy Division, Manufacturing Department, Central Metallurgical Research and Development Institute, Cairo 11422, Egypt;
3. Department of Production Technology, Faculty of Industrial Education, Beni-Suef University, Beni-Suef 62511, Egypt

Received 18 December 2013; accepted 16 June 2014

Abstract: The effect of iron addition on the microstructure, mechanical and magnetic properties of Al-matrix composite was studied. Mechanical mixing was used for the preparation of 0, 5%, 10% and 15% Fe−Al composites (mass fraction). Mixtures of Al−Fe were compacted and sintered in a vacuum furnace at 600 °C for 1 h. X-ray diffraction (XRD) of the samples containing 5% and 10% Fe indicates the presence of Al and Fe peaks, while sample containing 15% Fe reveals Al and $Al_{13}Fe_4$ peaks. The results show that both densification and thermal conductivity of the composites decrease by increasing the iron content. The presence of iron in the composite improves the compressive strength and the hardness. The strengthening mechanism is associated with the grain refinement of the matrix and uniform distribution of the Fe particles, as well as the formation of $Al_{13}Fe_4$ intermetallic. The measured magnetization values are equal to 0.3816×10^{-3} A·m^2/g for 5% Fe sample and increases up to 0.6597×10^{-3} A·m^2/g for 10% Fe sample, then decreases to 0.0702×10^{-3} A·m^2/g for 15% Fe sample. This can be explained by the formation of the diamagnetic $Al_{13}Fe_4$ intermetallic compound in the higher Fe content sample detected by XRD analysis.

Key words: Al−Fe composite; powder metallurgy; microstructure; mechanical properties; magnetic properties

1 Introduction

Aluminum matrix composites (AMCs) are one of the most demanding engineering materials in the category of metal matrix composites (MMCs) due to the combination of their light weight and excellent mechanical and tribological properties. These composites have been widely used for structural, and functional applications in automotive and aerospace industries [1−3]. The optimum properties of AMCs depend on good selection of the reinforcing phase and the processing technique/ parameters.

Powder metallurgy (P/M) route is one of the most widely used methods for producing AMCs due to its low processing costs as well as the ease and the accuracy to obtain near net shaped components of complex geometry. The most essential steps of P/M technique are mixing of powders, compaction, and sintering [4−6]. Compaction of loose powders under externally applied pressure and sintering of green compacts produced in earlier stage are the main processing parameters, and these parameters affect the density of the final product.

Al−Fe alloys are attractive for application at temperatures beyond those normally associated with conventional Al alloys because of the stability of the microstructure originating from the low diffusivity of Fe in Al. In addition, alloying Al with Fe increases its high temperature strength due to dispersion of second-phase particles [7]. The strengthening effect in Al−Fe alloys can be enhanced by increasing the solid solubility of Fe in Al matrix by nonequilibrium processing techniques [8−15].

In a comprehensive study, it was found that most of the earlier investigations related to Fe−Al binary phase system, were focused either on liquid-phase sintering and/or iron-rich composition (more than 20% Fe) [16]. Therefore, in the present investigation, an attempt has

Corresponding author: A. FATHY; Tel: +2-122-4048813; Fax: +2-55-2304987; E-mail: afmeselhy@zu.edu.eg
DOI: 10.1016/S1003-6326(15)63577-4

been made to examine the compaction and sintering behavior of Al-rich Al−Fe binary phase system. The aim of this work is the preparation of 0−15% Fe−Al metal matrix composites by P/M route. The major objective of the present investigation is to study the effect of Fe content on the physical, mechanical and magnetic properties of Al-matrix composites.

2 Experimental

2.1 Composite preparation

Commercially atomized aluminum powder with an average particle size of 20 μm and 99.7% purity (Fig. 1(a)) and Fe (99.5% purity and 10 μm in size) (Fig. 1(b)) were used as starting materials for composite fabrication. The appropriate amounts of Al with 5%, 10% and 15% Fe of the selected powders were thoroughly mixed in a conventional double-cone mixer at 180 r/min for 3 h to achieve homogenization and remove any clusters of powders. The powders were mixed with 0.5% paraffin wax as a lubricant to reduce friction during compaction, and liquid acetone was used as a process control agent. The mixed powders were dried at 80 °C for 30 min and cold compacted at room temperature in a uniaxial press at 500 MPa. The prepared green compacts were then dried for 30 min at 200 °C for complete removal of moisture, entrapped gases, and other impurities. Furthermore, sintering of all the green compacts was carried out using a ceramic tubular furnace in a vacuum atmosphere at 600 °C for 1 h and a heating rate of 10 °C /min.

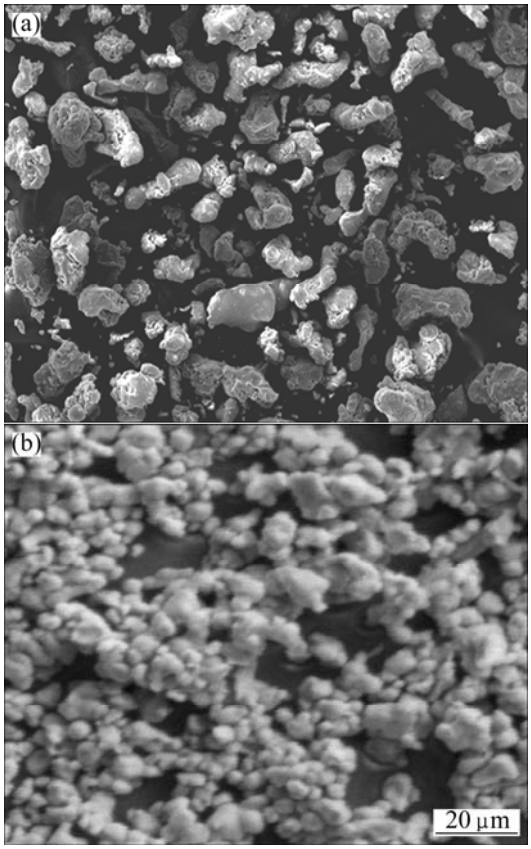

Fig. 1 SEM micrographs of elemental powders of aluminum (a) and iron (b)

2.2 Composite characterization

X-ray diffraction (XRD) analysis was carried out on a diffractometer model Burcker D8 Advance with Ni filtered and Cu target, K_α radiation. The crystallite size, the amount of dissolved Fe powders and the constituent phases of the sintered samples were estimated. True densities of the composites were measured by using the Archimedes' method (ASTM B962) and compared with the theoretical densities to obtain varying degree of densification. Electrical conductivity of the samples were measured and the thermal conductivity can be calculated according the Wiedemann-Franz law. The previous publication by the authors gave a detailed description of the procedures [17].

The microstructure of the prepared composites was examined by both optical model Olympus PMG 3−F3 microscope and scanning electron microscope (SEM, model: JEOL, JSM−5410). The elemental analysis of the specimens was performed using an energy dispersive spectroscopy (EDS) microanalyses equipped on scanning electron microscope (SEM). Hardness was measured using Vickers indentation technique with a load of 3 kg for a dwelling time of 10 s and an average of five readings was reported. The mechanical properties of the sintered samples were evaluated also by a compression test using a universal testing machine model HU−F500KN, according to standard ASTM E9. Cuboidal specimens of 2 mm × 2 mm × 4 mm at an initial strain rate of 1.0×10^{-3} s^{-1} at room temperature were used [18]. The compression experiments were terminated at 65% specimen strains.

The magnetic properties of investigated materials were measured using a 9600-1 LDJ vibrating sample magnetometer (VSM) in which the samples were vibrated at a constant frequency between a set of sense coils. As the magnetic field is varied through a specified range, the magnetic moment of the sample is measured by the sense coils with a lock-in amplifier. The dependency between the magnetization and magnetic field (hysteresis loop) for the prepared WHAs samples was measured. The measured properties included magnetic saturation (M_s), coercivity (H_c), permeability (μ_r) and remanence magnetization (retentivity) (M_r).

3 Results and discussion

3.1 X-ray diffraction analysis

Figure 2 shows the XRD patterns of pure Al, 5%, 10% and 15% Fe−Al composites. The XRD patterns for 5% and 10% Fe−Al composites show two types of peaks

that belong to Al and Fe elements. In the case of Al−15% Fe sample, the XRD peaks could be indexed as Al and $Al_{13}Fe_4$ phases, as shown in the patterns. From the phase diagram of Al−Fe, the ratio between Al and Fe in Al−15%Fe sample is sufficient for the formation of $Al_{13}Fe_4$ intermetallic which consumes all the Fe particles in the composite, as the type of intermetallic formed is found to be dependent on the Fe content, changing from Al_6Fe at 2.5%−10% Fe to $Al_{13}Fe_4$ at 15% Fe [19].

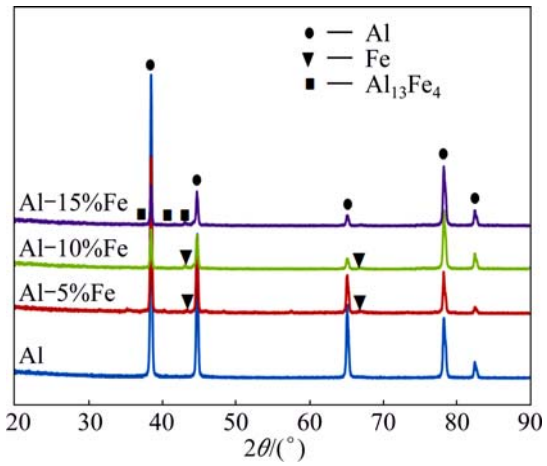

Fig. 2 XRD patterns of Al−Fe composites after sintering

As the Fe content increases, the intermetallic $Al_{13}Fe_4$ phase is formed according to the phase diagram between Al and Fe. This suggests that a solid-state reaction between Al and Fe during the sintering process occurs for the high Fe content sample [20,21], in which a brief study of earlier investigations related to Al−Fe binary system describes the formation of intermetallic compounds, produced by a variety of techniques like mechanical alloying and solid- and liquid-phase sintering. For example, OLSZ OWKA-MYALSKA et al [20] characterized the intermetallic compounds in Al−Fe metal matrix composite in the composition range of 3%−6% Fe (volume fraction) at hot pressing temperature of 630 °C for the time duration of 5−30 min. But they have not mentioned the chemical formula of the characterized intermetallic compound. One of the authors of the present investigation has already reported the formation of Al_3Fe intermetallics in the Al−Fe composites which were prepared by dispersion of Fe in aluminum melt by impeller mixing and bottom pouring chill casting technique [21]. The Fe content for the above investigation varies from 1.67% to 11.2%. This report suggests that the formation of intermetallics can also take place at low content of Fe in Al−Fe binary mixtures.

3.2 Effect of Fe content on densification

Bar graph illustrating the densification measured after compaction and sintering of the Al–Fe composites as a function of Fe content is shown in Fig. 3. It is clear that the theoretical density increases by increasing Fe content, which can be attributed to the higher density of Fe (7.8 g/cm^3) more than pure Al (2.7 g/cm^3). However, sintering of compacts at 600 °C for 1 h results in a densification (96.7%) for Al matrix, which decreases with the increase of Fe content and reduces to 92.3% for Al−15%Fe composite. This lower densification in 15% Fe−Al sample is due to the agglomeration of Fe particles during the sintering process with the increase of Fe content. During the sintering process, the Fe particles are distributed randomly due to its high melting point and high density. The dense network formed by Fe particles prevents the densification [22]. In addition, the decline in the pressing capacity of samples with increasing in the amount of Fe is due to the high hardness of Fe. Therefore, these composites have lower compressibility that results in lower densification.

3.3 Effect of Fe content on thermal conductivity

Figure 4 shows that the thermal conductivity of Al and Al–Fe composites depends on the content of Fe.

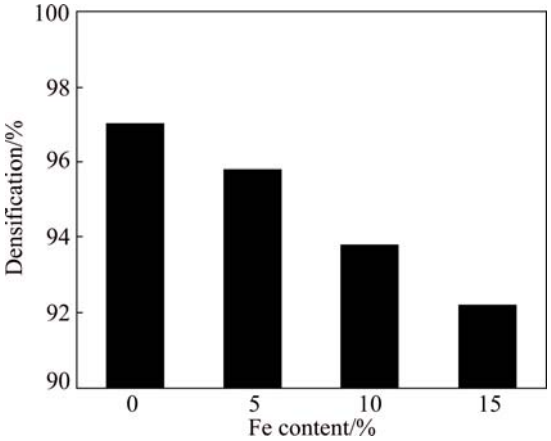

Fig. 3 Bar graph of densification of Al−Fe composites as function of Fe content

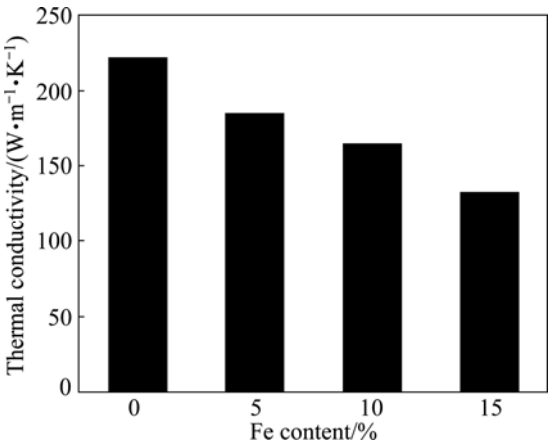

Fig. 4 Bar graph of thermal conductivity of Al−Fe composites as function of Fe content

Thermal conductivity of composites decreases with increasing content of Fe. This is attributed to the thermal conductivity of Fe which is lower so far than that of Al. The second reason is the agglomeration of some Fe particles at the grain boundaries which can form a kind of grain boundary phase that increases the scattering of the charge carrier, hence reducing the thermal conductivity. Thermal conductivity of the metal is mainly dependent on the movement of the internal electron. Fe particles can increase the scattering surfaces for the conduction electrons in the matrix and reduce the thermal conductivity of the Al matrix composites.

The conductivity of two-phase composites is determined by many factors, such as: 1) the conductivities of the constituent phases; 2) the volume fractions and distributions of the constituent phases; 3) the size, shape, orientation and spacing of the phases; 4) interaction between phases; and 5) the preparation method [23].

3.4 Metallographic analysis

Figure 5 shows the optical micrographs of composites with 5%, 10% and 15% Fe, revealing the presence of larger amount of second dispersed phase particles. Micrographs show the homogeneous dispersion of Fe in the Al matrix for the three Fe−Al composites. Micrographs also show irregularly shaped Fe−Al composite particles. It is clear that chains of particles and particles aggregation are seen and concentrated at the grain boundaries of the Al particles. Most particles show a continuous iron phase. Also, the micrographs contain three phases, one of them is the gray light which is the Al matrix and the dispersed phase is the gray spots which represent the Fe particles, and the third phase is the black spots which are the pores in the sintered samples. All the composites were also studied under SEM for further investigation of the microstructures.

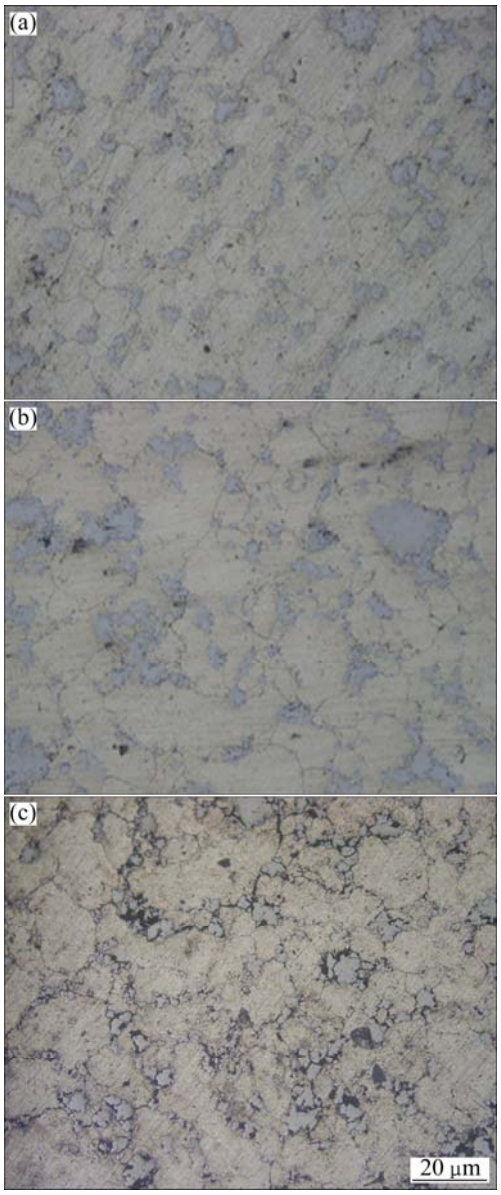

Fig. 5 Optical micrographs of Al−5%Fe (a), Al−10%Fe (b), and Al−15%Fe (c) composites

Figure 6 shows the SEM images of 0, 5%, 10% and 15% Fe−Al composites sintered at 600 °C for 1 h, in which the distribution of Fe in Al matrix can be easily seen. Microstructure of the composites reveals small discontinuity and a reasonably uniform distribution of Fe particles in the aluminum matrix. The ceramic phase is shown as dark phase, while the metal phase is white. It is clear from Fig. 6(a) that Al particles exist in rounded to sub-rounded coarse grains with black lines represented the grain boundaries. It is also noticed in Figs. 6(b)−(d) that very tiny iron particles are distributed throughout the aluminum matrix along the grain boundaries. Also, reduction of porosity along the grain boundaries and residual porosity within grains are observed. Fe particles make agglomerations at the grain boundaries of Al particles, but by increasing Fe contents (for 15% sample), the Fe particles are dispersed all over the Al matrix. The dispersed phase all over the Al matrix represents the formation of an intermetallic phase between Al and Fe which is $Al_{13}Fe_4$ confirmed by XRD results.

The EDS profile corresponding to the microstructures is also given as an evidence of elements presented in the sintered 15% Fe−Al sample. Figure 7 illustrates the points at which EDS is performed, and the intensity of peaks is corresponding to the elements presented at that point. The existence of elements in all possible phases such as presence of Fe in Al matrix and Al in Fe particle is shown in Figs. 7(a) and (b), respectively. The EDS result of tiny particles shows that both Al and Fe phases are presented, which indicates the

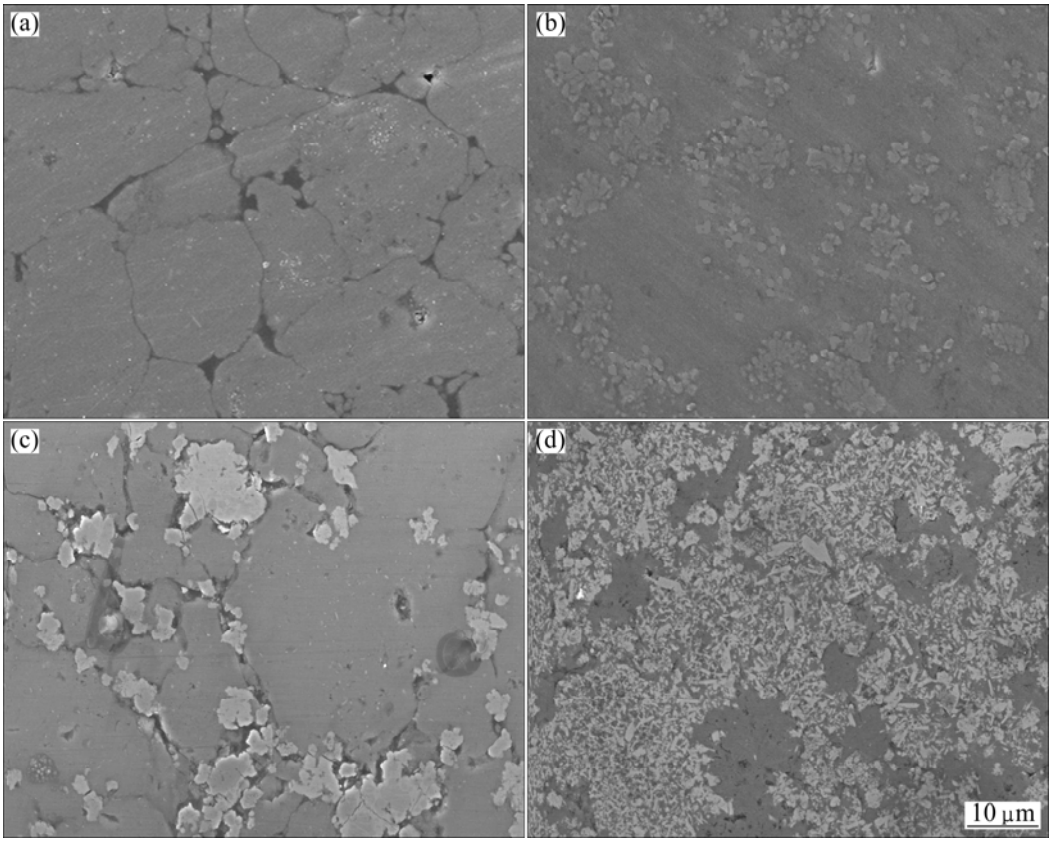

Fig. 6 SEM micrographs of Al (a), Al−5%Fe (b), Al−10%Fe (c) and Al−15%Fe (d) composites

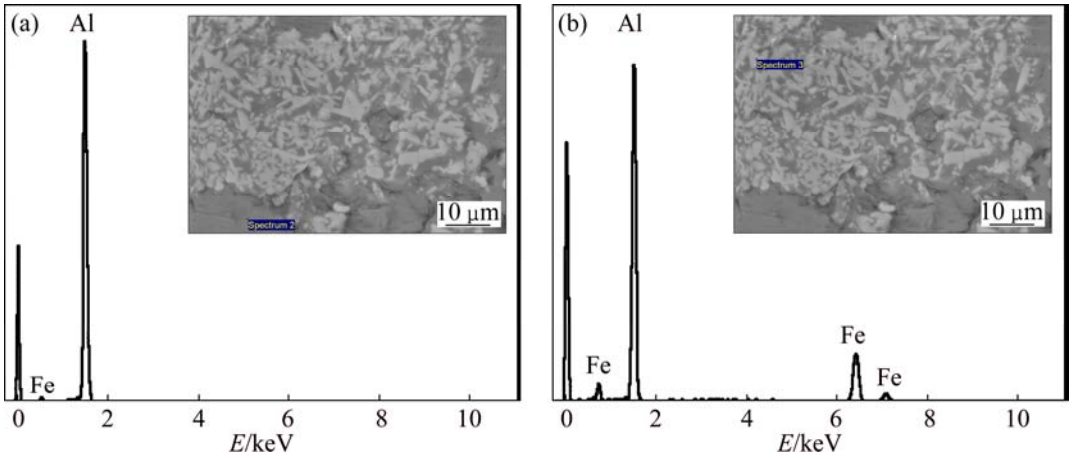

Fig. 7 EDS spot results of sintered Al−Fe metal matrix composites: (a) Al matrix; (b) Fe particle

presence of the intermetallic $Al_{13}Fe_4$ all over the Al matrix.

3.5 Effect of Fe content on hardness

Bar graph illustrating the hardness measured after compaction and sintering of the Al–Fe composites as a function of Fe content is shown in Fig. 8. The measured hardness values indicate a continuous increase in hardness with increasing Fe content from 0 up to 15%. The hardness of material is a physical parameter indicating the ability of resisting local plastic deformation. Fe with high hardness, which acts as a reinforcing phase, is dispersed in Al matrix and obstacles the movement of dislocation when plastic deformation occurs. The maximum hardness value is obtained for Al−15% Fe composite which is about HV 65 and the minimum value is HV 32 for Al matrix. The hardness of Al is improved considerably with the addition of Fe particles at the expense of its ductility that can be attributed to high hardness of Fe. Also, for 15% Fe sample, the formation of the intermetallic $Al_{13}Fe_4$ increases the hardness of the composite. This result is consistent with the results of Ref. [24].

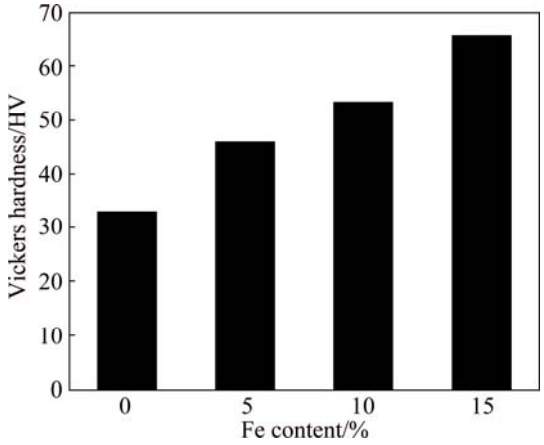

Fig. 8 Bar graph of hardness of Al−Fe composites as a function of Fe content

3.6 Effect of Fe content on compressive strength

In the attempt to evaluate the mechanical properties of the composites, compression test was conducted at room temperature under uniaxial compressive loading and the stress–strain curves are shown in Fig. 9. Obviously, the compressive strength value of Al−Fe composite is significantly higher than that of the Al matrix, suggesting that the Fe particles can strongly enhance the mechanical strength of the Al matrix. In particular, Al−15% Fe composite exhibits compressive strength of about 550 MPa combined with an appreciable plastic strain about 65%. Although tensile testing can determine if a proper bonding has been produced yet, compression test can also be helpful to studying the barreling and upsetting behavior of the compacts. Stronger bonds among particles delay the crack initiation during deformation especially at the time of barreling [25,26].

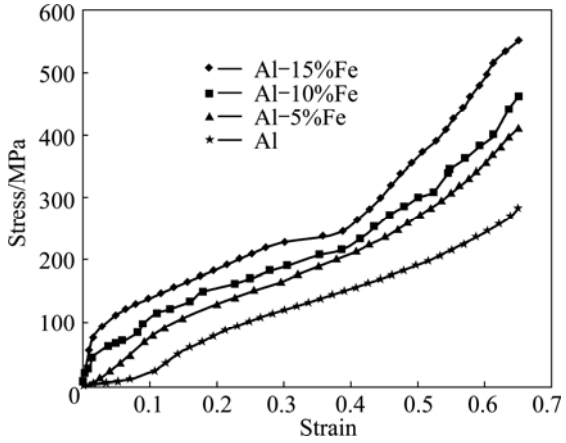

Fig. 9 Stress–strain curves of Al−Fe composites

Also, it can be observed that by increasing the amount of Fe from 0 to 15%, the compressive strength increases from 283 to 550 MPa. This is attributed to the effect of Fe particles as they prevent the movement of dislocations in pure Al matrix through dispersion strengthening mechanism [27]. Also the compressive strength increases for 15% Fe sample due to the formation of $Al_{13}Fe_4$ intermetallic compound which was detected by XRD. ANGERS et al [28] have reported a tensile strength of 514 MPa and elongation of 5.2% for Al−2024/7.4% SiC composite, which was produced by a combination of mechanical milling and hot extrusion. Compared with the previous results, our materials have a better combination of strength and ductility, indicating that the metallic glass particles significantly improve the mechanical behavior of the MMCs.

3.7 Effect of Fe content on magnetic properties

In this work, the magnetic properties of 5%, 10% and 15% Fe−Al composites were examined. The dependence between the magnetic field (H) and magnetization (M) (hysteresis loop) was measured at room temperature. The measured B−H hysteresis loops are shown in Fig. 10. The values of magnetization (M_s), coercivity (H_c), permeability (μ_r) and remanence magnetization (M_r) are recorded in Table 1. The values of the magnetic saturation (M_s) reveal the presence of the ferromagnetic iron phase. The shape of the registered loops, as well as the values of magnetization, indicates the magnetic properties of the samples. At room temperature, for the applied field 1600 km/A, the measured magnetization value is equal to 0.3816×10^{-3} $A\cdot m^2/g$ for 5% Fe sample and increases up to 0.6597×10^{-3} $A\cdot m^2/g$ for 10% Fe sample and then decreases to 0.0702×10^{-3} $A\cdot m^2/g$ for 15% Fe sample. This can be explained by the formation of an intermetallic compound between Al and Fe in the high Fe content sample as shown from XRD analysis, in which Fe loses its magnetization due to the formation of the intermetallic $Al_{13}Fe_4$. The ratio of Fe phase in the three samples (5%, 10% and 15%) has an effect on improving

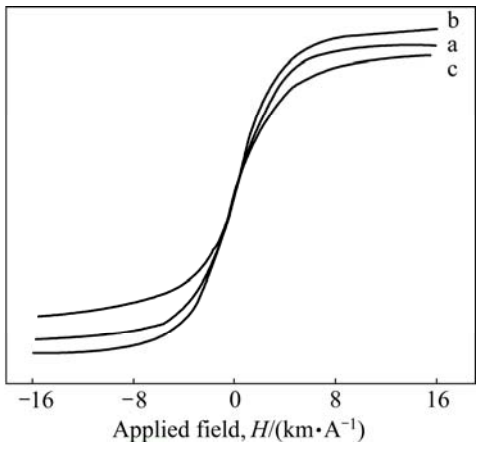

Fig. 10 Magnetization curves (Hysteresis loops) of Al−Fe composites: (a) 5% Fe; (b) 10% Fe; (c) 15% Fe

Table 1 Magnetic property of produced Al-Fe composites

Samples	Magnetic properties		
	$M_s/(10^{-3}A\cdot m^2\cdot g^{-1})$	$H_c/(m\cdot A)$	$M_r/(10^{-3}A\cdot m^2\cdot g^{-1})$
Al−5%Fe	3.816	2502.48	0.0027576
Al−10%Fe	0.6597	2450.56	0.0053166
Al−15%Fe	0.0702	6228.16	0.0017923

the magnetic properties of Al matrix composites. The saturation magnetization (M_s), is an intrinsic property independent on the grain size and microstructure, and dependent only on the composition of the alloy (decreases as the amount of aluminum increases). Conversely, coercivity H_c, and remanence M_r, can be regarded as extrinsic properties dependent on both grain size and microstructure, as well as grain shape, texture, and internal stress [29]. The results also show that the value of coercivity (H_c) for Al−15%Fe sample is higher than that of Al−10%Fe and Al−5%Fe composites. This may be attributed to the relatively fine microstructure of Al−15% Fe composite.

4 Conclusions

1) Fe particles reinforced Al-matrix composites are successfully obtained and consolidated by powder metallurgy technique.

2) X-ray results indicate the formation of supersaturated solid solution of Fe in Al matrix containing 5%−10% Fe, while Al−15%Fe composite forms an intermetallic $Al_{13}Fe_4$.

3) It can be observed from the present investigation that Fe could be uniformly distributed in aluminum. A significant increase in the mechanical properties of the composites compared to the matrix is achieved at the cost of only slight increase in density.

4) The maximum hardness and compressive strength of Al−15%Fe composite are HV 65 and 550 MPa, respectively, while retaining a considerable deformation of about 65%, leading to a remarkable combination of high strength and good plasticity.

5) The improvement of mechanical properties is attributed to the formation of intermetallic $Al_{13}Fe_4$, the grain refinement and the uniformly distribution of the Fe particles.

References

[1] SURAPPA M K. Aluminum matrix composites: Challenges and opportunities [J]. Sadhana, 2003, 28: 319−334.

[2] MOHAN S, SRIVASTAVA S. Surface behavior of as cast Al−Fe intermetallic composites [J]. Tribology Letters, 2006, 22: 45−51.

[3] HEINZ A, HASZLER A, KEIDEL C, MOLDENHAUER S, BENEDICTUS R, MILLER W S. Recent development in aluminum alloys for aerospace applications [J]. Materials Science and Engineering A, 2000, 280: 102−107.

[4] TORRALBAA J M, DA COSTAB C E, VELASCO F. P/M aluminum matrix composites: An overview [J]. Materials Processing Technology, 2003, 133: 203−206.

[5] PICKENS J R. Aluminum powder metallurgy technology for high-strength applications [J]. Materials Science, 1981, 16: 1437−1457.

[6] LIU Y B, LIM S C, LU L, LAI M O. Recent development in the fabrication of metal matrix-particulate composites using powder metallurgy techniques [J]. Materials Science, 1994, 29: 1999−2007.

[7] FROES F H, SENKOV O N, BABURAJ E G. Synthesis of nanocrystalline materials-an overview [J]. Materials Science and Engineering A, 2001, 301: 44−53.

[8] HUANG B, TOKIZANE N, ISHIHARA K N, SHINGU P H, NASU S. Amorphization of Al−Fe alloys formed by ball milling and repeated rolling [J]. Non-crystalline Solids, 1990, 117−118: 688−691.

[9] MUKHOPADHYAY D K, SURYANARAYANA C, FROES F H. Structural evolution in mechanically alloyed Al−Fe powders [J]. Metallurgical and Materials Transactions A, 1995, 26: 1939−1946.

[10] MURTY B S, RANGANATHAN S. Novel materials synthesis via mechanical alloying [J]. International Materials Review, 1998, 43: 101−141.

[11] SASAKI T T, OHKUBO T, HONO K. Microstructure and mechanical properties of bulk nanocrystalline Al−Fe alloy processed by mechanical alloying and spark plasma sintering [J]. Acta Materialia, 2009, 57: 3529−3538.

[12] FADEEVA V, LEONOV A V. Formation of Al−Fe supersaturated solid solution by mechanical alloying [J]. Materials Science Forum, 1992, 90: 481−488.

[13] BAYRAKTAR E, KATUNDI D. Development of a new aluminum matrix composite reinforced with iron oxide [J]. Achievements in Materials and Manufacturing Engineering, 2010, 38: 7−14.

[14] MAZAHERY A, SHABANI M O. Study on microstructure and abrasive wear behavior of sintered Al matrix composites [J]. Ceramics International, 2012, 38: 4263−4269.

[15] MAZAHERY A, SHABANI M O. Nano-sized silicon carbide reinforced commercial casting aluminum alloy matrix: Experimental and novel modeling evaluation [J]. Powder Technology, 2012, 217: 558−565.

[16] KANG H Z, HU C T. Swelling behavior in reactive sintering of Fe−Al mixtures [J]. Materials Chemistry and Physics, 2004, 88: 264−272.

[17] FATHY A, EL-KADY O. Thermal expansion and thermal conductivity characteristics of Cu−Al_2O_3 nanocomposites [J]. Materials and Design, 2013, 46: 355−359.

[18] FATHY A, SHEHATA F, ABDELHAMEED M, ELMAHDY M. Compressive and wear resistance of nanometric alumina reinforced copper matrix composites [J]. Materials and Design, 2012, 36: 100−107.

[19] NAYAK S S, MURTY B S, PABI S K. Structure of nanocomposites of Al−Fe alloys prepared by mechanical alloying and rapid solidification processing [J]. Bull Mater Sci, 2008, 31: 449−454.

[20] OLSZ ´OWKA-MYALSKA A, SZALA J, CWAJNA J. Characterization of iron aluminides formed in situ in an aluminum matrix composite [J]. Materials Characterization, 2006, 56: 379−383.

[21] MOHAN S, SRIVASTAVA S. Surface behavior of as cast Al−Fe intermetallic composites [J]. Tribology Letters, 2006, 22: 45−51.

[22] SHEN Y L, CHAWLA N. On the correlation between hardness & tensile strength in particle reinforced metal matrix [J]. Materials Science and Engineering A, 2001, 297: 44−47.

[23] EL-KADY O, FATHY A. Effect of SiC particle size on the physical and mechanical properties of extruded Al matrix nanocomposites [J].

Materials and Design, 2014, 54: 348−353.
[24] KHRAISAT W, ABU JADAYIL W. Strengthening aluminum scrap by alloying with iron [J]. Jordan Journal of Mechanical and Industrial Engineering, 2010, 4: 372−377.
[25] NARAYANASAMY R, RAMESH T, PANDEY K S. Workability studies on cold upsetting of Al−Al_2O_3 composite material [J]. Materials and Design, 2006, 27: 566−575.
[26] NARAYANASAMY R, RAMESH T, PANDEY K S. Effect of geometric work-hardening and matrix work-hardening on workability and densification of aluminum–3.5% alumina composite during cold upsetting [J]. Materials and Design, 2008, 29: 1582−1599.
[27] DIETER G E. Mechanical metallurgy [M]. 3rd ed. New York: McGraw-Hill, 1976.
[28] ANGERS R, KRISHNADEV M R, TREMBLAY R, CORRIVEAU J F, DUBE D. Characterization of SiC_p/2024 aluminum alloy composites prepared by mechanical processing in a low energy ball mill [J]. Materials Science and Engineering A, 1999, 262: 9−15.
[29] KAW A K. Mechanics of composite materials [M]. 2nd ed. New York: Taylor & Francis Group, 2006: 40−46.

铁对粉末冶金法制备铝基复合材料微观组织和力学性能及磁学性能的影响

A. FATHY[1], Omyma EL-KADY[2], Moustafa M. M. MOHAMMED[3]

1. Department of Mechanical Design and Production Engineering, Faculty of Engineering, Zagazig University, Zagazig 44519, Egypt;
2. Powder Metallurgy Division, Manufacturing Department, Central Metallurgical Research and Development Institute, Cairo 11422 Egypt;
3. Department of Production Technology, Faculty of Industrial Education, Beni-Suef University, Beni-Suef 62511, Egypt

摘　要：研究铁对粉末冶金法制备铝基复合材料微观组织、力学性能及磁学性能的影响。利用机械混合制备含 0, 5%，10%和 15% Fe(质量分数)的铝基复合材料。Al−Fe 混合粉末经压制后在真空炉中 600 °C 烧结 1 h。XRD 结果表明：在含有 5%和 10% Fe 的试样中只有 Fe 和 Al 的衍射峰，而含有 15% Fe 的试样中则存在 Al 和 $Al_{13}Fe_4$ 的衍射峰。实验结果表明：随着 Fe 含量的增加，材料的致密度和导热性变差。复合材料中的 Fe 可以提高其强度和硬度。材料的强化机制包括基体的晶粒细化，Fe 颗粒的均匀分布以及 $Al_{13}Fe_4$ 金属间化合物的形成。含有 5% Fe 试样的磁化强度为 $0.3816\times10^{-3}A\cdot m^2/g$，对于含有 10%Fe 的试样，其磁化强度增加至 $0.6597\times10^{-3}A\cdot m^2/g$，而对于含有 15% Fe 试样，其磁化强度降低至 $0.0702\times10^{-3}A\cdot m^2/g$。这是由于在高铁试样中形成了反磁性的 $Al_{13}Fe_4$ 金属间化合物导致磁化强度降低。

关键词：Al−Fe 复合材料；粉末冶金；微观组织；力学性能；磁学性能

(Edited by Yun-bin HE)